Sci. J. Fac. Sci. Minufia Univ., 2009, Vol.XXIII(2).149 - 170

MINERALOGICAL CHARACTERISTICS OF THE SEPARATED MAGNETIC RUTILE OF THE EGYPTIAN BLACK SANDS

MOHAMED ISMAIL MOUSTAFA
Nuclear Materials Authority
Email: ismail2251962@yahoo.com

ABSTRACT

The Egyptian black sands contain several economic minerals; the most important are ilmenite, magnetite, garnet, zircon, rutile and monazite. During the concentration and separation of a high–grade rutile concentrate, a bulk magnetic fraction was obtained and composes mainly of individual titanhematite grains, ferriilmenite–titanhematite exsolved intergrowthed grains, magnetic leucoxene, chromite and magnetic rutile. The latter represents 6 wt. % of the bulk magnetic fraction or ≈ 4 wt. % of the original rutile content in the raw sands. Most of the magnetic rutile varieties are primary rutile grains contaminated with opaque zones present as inclusions, staining–coating and/or forming with rutile composite locked grains. These rutile varieties have magnetic characters range from strong-moderate paramagnetic to very weak paramagnetic. Twenty three polished grain surfaces representing most of the magnetic rutile varieties were investigated using Cameca SX-100 electron microprobe where 193 spots were analyzed. The calculation of the average chemical composition of the identified magnetic rutile especially for TiO_2, Fe_2O_3, SiO_2, Al_2O_3, CaO and Cr_2O_3, gives 66.34%, 21.71%, 6.39%, 1.8%, 1.19%, and 0.1%, respectively. According to the obtained microprobe chemical analyses, the magnetic rutile varieties were found to consist rutile, titanhematite, pseudorutile, leached pseudorutile, and ilmenite in a decreasing order of abundance. Some inclusions were also detected in the different magnetic rutile varieties. They are composed most probably of garnet, silicon dioxide, amphibole, ilmenite, feldspar, mica and zircon. These inclusions reflect the derivation of magnetic rutile from various crystalline igneous and metamorphic rocks. The mass magnetic susceptibilities of the various investigated magnetic rutile varieties are governed by the associated mineral species and size of their corresponding zones in comparison to the rutile mineral component, in addition also to both of type and size of the associated mineral inclusions. If the content of the magnetic rutile varieties are included inside the final high grade rutile concentrate, it will affect the marketable specification and hence its salable prices. These magnetic primary rutile varieties are recommended to be blended with magnetic leucoxene or some types of the Egyptian beach ilmenite concentrates to improve their overall marketable specifications especially for both of Ti, Fe and Cr contents.

Key words:

Magnetic rutile, magnetic susceptibility, pseudorutile, titanhematite, exsolution intergrowths.

INTRODUCTION

The Egyptian black sands extend along the Mediterranean coast from Abu Qir to the west, to Rafah to the east. Most of these deposits are present now either as beach sediments or sand dunes. The east Rosetta area contains relatively enriched beach black sands. Rutile content in these beach black sands ranges from 0.05wt. % in the most upper meter to 1.5wt. % in the naturally highly concentrated surfacial beach black sands (maximum depth of 20 cm) in the eroded areas.

Many authors delt with studying the mineralogical characters of the Egyptian beach rutile e.g. El Hinnawi (1964); Kamel (1964); Zaghloul and Kamel (1966); Hammoud (1966 & 1973); The Egyptian black sand's company (1969); Dabbour (1980 & 1997); Mohamed (1987); Naim et al. (1994); Moustafa (1995 & 1999); Dewedar (1998); Bishady et al. (2004) and others.

Kamel (1964) stated that "leucoxene, ilmenite and/or hematite replacements have been recorded among some of the altered rutile grains". He explained that leucoxene commonly occurs in irregular patches in some rutile grains, while each of ilmenite or hematite is rare. Kamel (op. cit.) also explained that minute opaque iron ore crystals, zircon-like crystals and gas cavities are the different recorded inclusions in rutile grains of Rosetta black sands.

Hammoud (1973) explained that the ferriferous rutile variety represents 4.2% of the Egyptian beach rutile concentrate, and most of the particles were found to be composite in nature; displaying exsolution intergrowths and granular aggregates in polished sections. The exsolution intergrowths consist of rutile–ilmenite, rutile–hematite and rarely ilmenite–rutile. On the other hand, the granular aggregates composed mainly of rutile and ilmenite in an irregular or oriented way.

Using both of wet-gravity concentration, high-tension electrostatic separation and both low and high intensity magnetic separation techniques, most of the individual economic mineral concentrates from the Egyptian black sands can be obtained with marketable grades and accepted recoveries (Hammoud, 1966, 1973 and Moustafa, 1999, 2003 and 2007).

In the present work, 100 tons of raw sands were collected from the most top meter from an area located after 7 km to the east of Rosetta estuary (Fig. 1). Using the flowsheet shown in Fig. (2), a final high–grade rutile concentrate assaying 99.3% with an overall recovery of 88.2% was obtained in the final non–magnetic fraction (Fig. 2).

In this paper, the optimum adjustment of operating conditions for the high–intensity magnetic separator, to remove most of the magnetic rutile varieties affecting the quality of the magnetically upgraded final rutile concentrate was predicted. Both of the chemical analysis, the identified corresponding mineral components and some of the associated inclusions were detected for 23 grains representing the various magnetic rutile varieties.

TECHNIQUES & METHODS

TECHNIQUES

Concentration and separation equipments

Utilizing the differences in physical properties between the different Egyptian economic beach minerals, the collected raw sands were processed using the following equipments: the Full size Wilfley shaking tables for wet-gravity concentration, the

Carpco (HP 167) high-tension roll-type electrostatic separator for high tension electrostatic separation, the Reading cross--belts magnetic separator, the Carpco (MIH

13-231-100) industrial high intensity induced roll magnetic separator, and the laboratory Carpco (ML H 13-111-5) high intensity lift-type magnetic separator for magnetic separation.

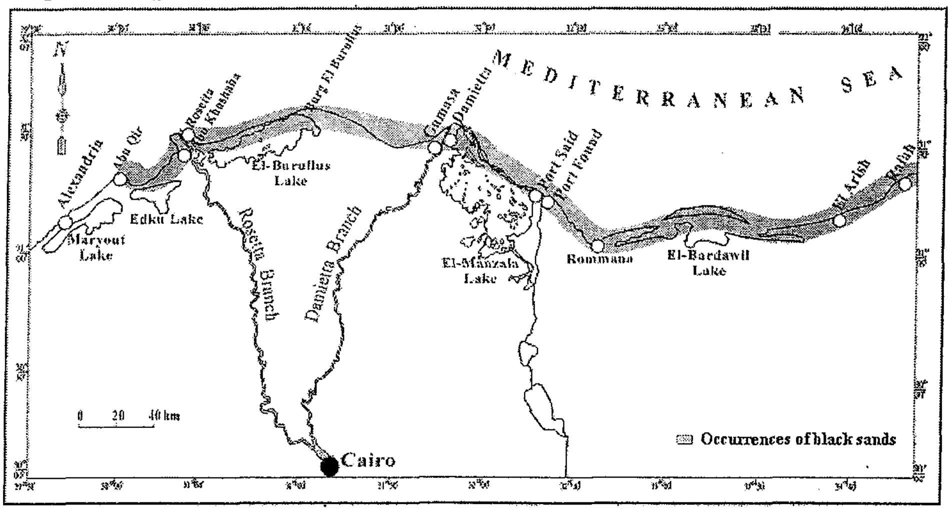

Fig. 1: Map showing the occurrences of the Egyptian black sands along the Mediterranean coast of Egypt.

Microprobe analysis

The polished sections of the identified magnetic rutile varieties were examined by electron microprobe analyzer, using the Cameca SX-100 electron microprobe analyzer (EMPA), in the Institute of Mineralogy and Crystal Chemistry, Stuttgart University, Germany The microprobe instrument is equipped with three wavelength dispersive spectrometers (WDS) and an energy dispersive spectrometer (EDS). The whole surface of the polished sections was examined by back scattered electron (BSE) images so that most of magnetic rutile grains with e.g. 10 μm size; or even smaller could be detected. The analytical conditions were 15 kv accelerating voltage; 15nA electron current; 180S counting time for each analyzed spot in the investigated grains and a focused electron beam diameter of 1 to 4 μm. The following standards were used: diopside for Mg and Ca, albite for Na, Corundum for Al, orthoclase for Si and K, rutile for Ti, rhodonite for Mn, Fe_2O_3 for Fe, zircon for Zr, Hf for Hf, Cr_2O_3 for Cr and sphalerite for Zn. Lines used for analysis were Lα for Zr, Mα for Hf and Kα for each of the other analyzed elements.

Polished sections and binocular microscope were also used for investigating the studied magnetic rutile.

METHODS

The Separation of magnetic rutile varieties.

The collected raw sands which contain 0.07% rutile were screened using a 1 mm screen aperture, to remove the coarse materials (+1mm). The undersized fraction was deslimed, that the deslimed raw sands were concentrated using the available shaking tables where considerable contents of the gangue minerals including amphiboles and pyroxenes (green silicates) in addition to quartz were removed in a final tailing fraction (Fig. 2). The tabled concentrate contains 1.2% rutile and most of the other economic beach minerals. Magnetite can be removed using the low intensity magnetic drum separator. The non–magnetic fraction was treated using Reading cross–belts magnetic separator where most of ilmenite and garnet are obtained in the various magnetic fractions (Fig. 2), while both of zircon, rutile and monazite in addition to some of green silicates and remaining quartz are obtained in the non–magnetic fraction (Fig. 2). The non–magnetic fraction containing 5.8% rutile was subjected to a circuit of shaking tabling to remove the majority of the associated gangue minerals in a final tailing fraction. The obtained tabled concentrate containing 11.45% rutile, was subjected to a circuit of high–tension electrostatic separation where most of zircon and monazite are obtained in the non–conductor fraction, while most of the rutile is obtained in the final conductor fraction. Rutile represents 54.4 wt. % of that fraction. To remove most of the magnetic contaminants associated with rutile, including primary magnetic rutile varieties, individual titanhematite grains, ferriilmenite-titanhematite exsolved intergrowthed grains, magnetic leucoxene, and chromite, the conductor rutile fraction was subjected to three stages of magnetic separation using the industrial high–intensity induced roll magnetic separator. The concluded optimum adjustment of operating conditions is as follows: 10 mm air gap of the escalping magnet and 6 mm air gap for each of the second and the third magnets.

The feeding rate was one ton/hour, the used ampere was 4 and the rotor speed was 160 r.p.m. Most of the hematite and magnetic leucoxene in addition to minor rutile varieties are dominated in both of the obtained first and second magnetic fractions. The majority of magnetic rutile varieties are dominated in the obtained third magnetic fraction. The magnetic rutile varieties represent 6 wt. % of the obtained successive three magnetic fractions and ≈ 4% of the original rutile content.

RESULTS AND DISCUSSION

Investigating the magnetic rutile varieties under the binocular microscope indicates that most of these grains are composed of primary rutile zones characteristic by transparent to translucent dark red, red, orange and yellow colours (Fig. 3). The grains contain small to large opaque inclusions, coatings or staining parts. Other grains seem to be composite of rutile and opaque materials (Fig. 3).

The identified mineral varieties:

Trying to differentiate between the magnetic rutile varieties, a representative sample of the bulk magnetic fraction was taken and magnetically differentiated using the laboratory lift–type high–intensity magnetic separator at a definite adjustment of operating conditions and using ampere values of 0.4, 0.8, 1.5 and 3. A representative sample of each obtained magnetic fraction was taken and the magnetic rutile varieties were picked, polished and investigated.

Six grains (G1 to G6, Fig. 4) of the 0.4 ampere magnetic fraction, eight grains (G7 to G14, Fig. 5) of the 0.8 ampere magnetic fraction, four grains (G15 to G18, Fig. 6) of the 1.5 ampere magnetic fraction and five grains (G19 to G23, Fig. 6) of the 3 ampere magnetic fraction were investigated.

The detected spots in the investigated grains were analyzed for Na_2O, K_2O, CaO, Al_2O_3, SiO_2, TiO_2, MnO, MgO, Cr_2O_3, ZnO, ZrO_2, HfO_2 and Fe. Iron was calculated as FeO in case of the identified ilmenite spots, while it was calculated as Fe_2O_3 allover other identified cases. The obtained results are shown in Table (1) and are summarized in Table (2).

It was detected that most of the analyzed spots in the rutile mineral components are almost homogenous and composed mainly of TiO_2 (mostly more than 98% TiO_2). Minor spots have appreciable contents of Al_2O_3 or Fe_2O_3.

The 0.4 ampere magnetic fraction:

The investigated grains are composed of rutile (G1); rutile, pseudorutile and altered ilmenite (G2); rutile and pseudorutile (G3); rutile and titanhematite including lamellae of pseudorutile and pseudobrookite (G5) and rutile and titanhematite including exsolved ferriilmenite, G6 (Fig. 4 & Table 1).

The G4 grain was identified as sphene replacing for ilmenite; containing a relatively high content of MnO, 8.2 and 7.11 Wt. % respectively (spots 21 and 22, Fig. 4 & Table 1). Mikhail (1971) explained that complete absence of either cavities or cracks between ilmenite and sphene indicates that the replacement process took place

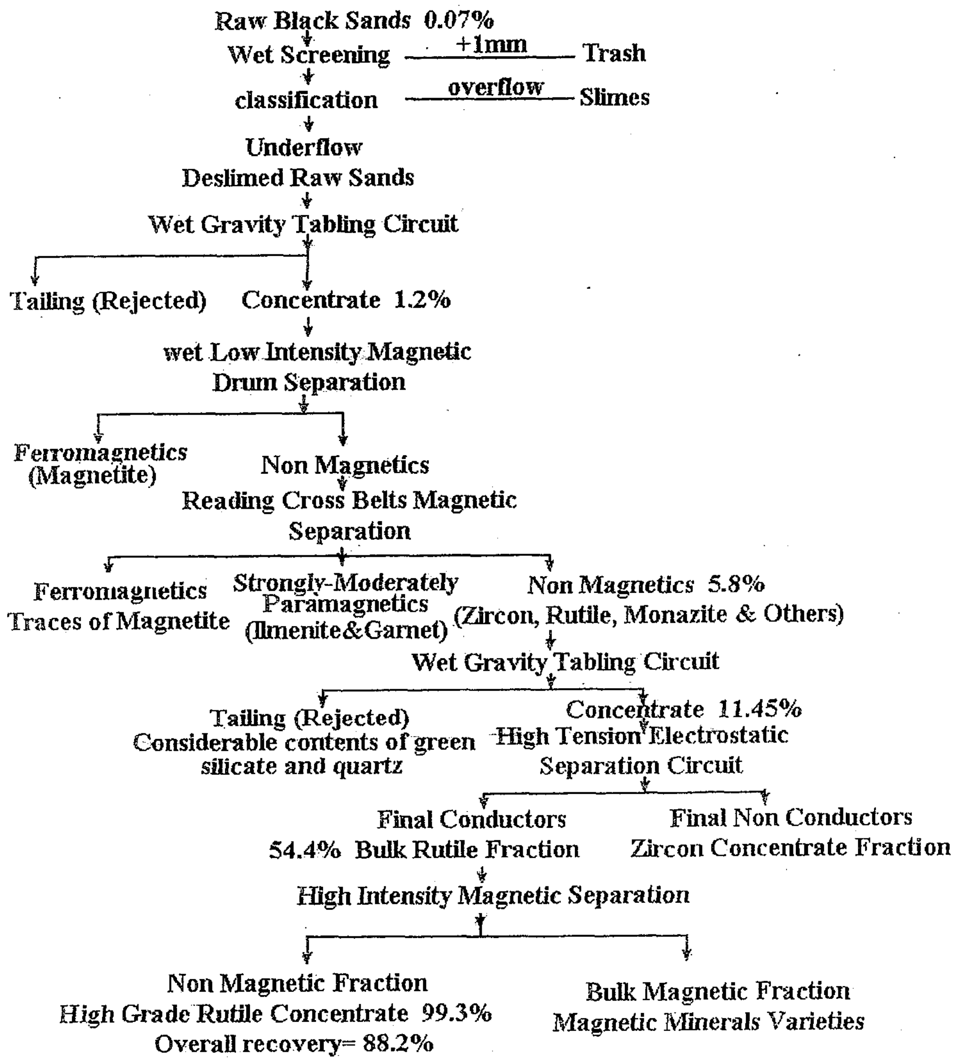

Fig. (2): A simplified flowsheet showing the various concentration and separation steps for obtaining the high–grade Egyptian beach rutile concentrate and the bulk magnetic fraction. The given percentages are corresponding to the rutile grades in each of the obtained fractions.

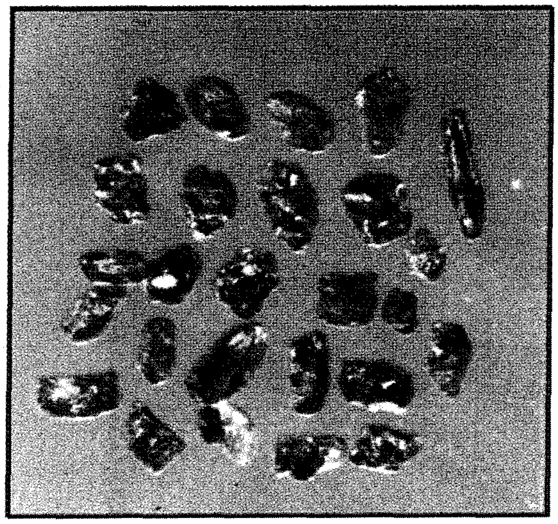

Fig. (3): Dark red, red, orange and yellow primary magnetic rutile grains associated with opaque regions of different sizes, shapes, and orientations. Binocular .microscope, X 60

volume by volume. According to Ramdohr (1940, 1956), sphene is developed by magmatic resorption or hydrothermal action.

It seems that the pseudorutile of G3 is due to rapid high temperature alteration affecting preexisting ilmenite. The reasons are almost constant chemical composition as regards to TiO_2, Fe_2O_3, MnO and Cr_2O_3 and the smooth boundary betweenpseudorutile and .rutile

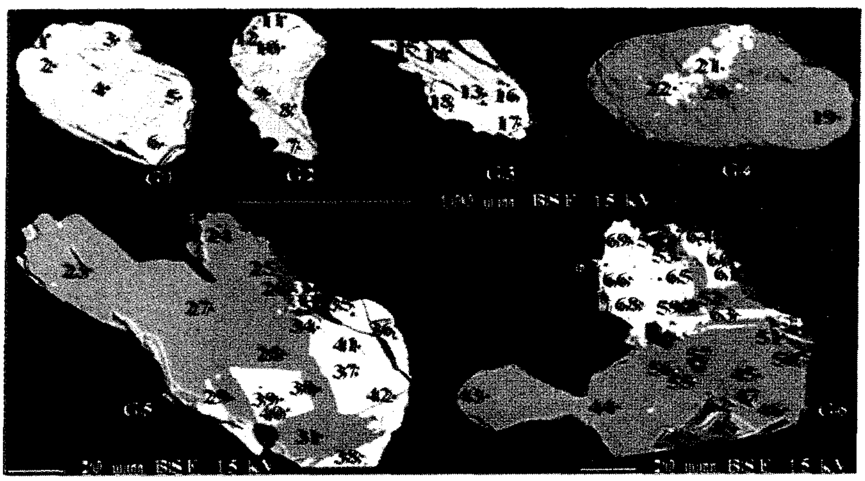

Fig. (4): Back scattered electron images (BSE) of the investigated magnetic rutile grains from the obtained 0.4 ampere magnetic fraction.

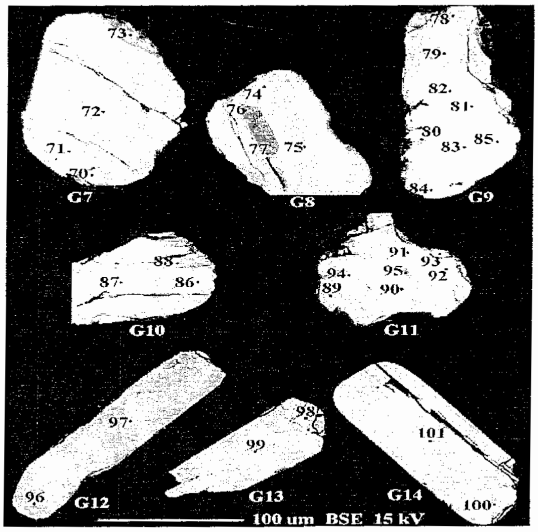

Fig. (5): Back scattered electron images (BSE) of the investigated magnetic rutile grains from the obtained 0.8 ampere magnetic fraction.

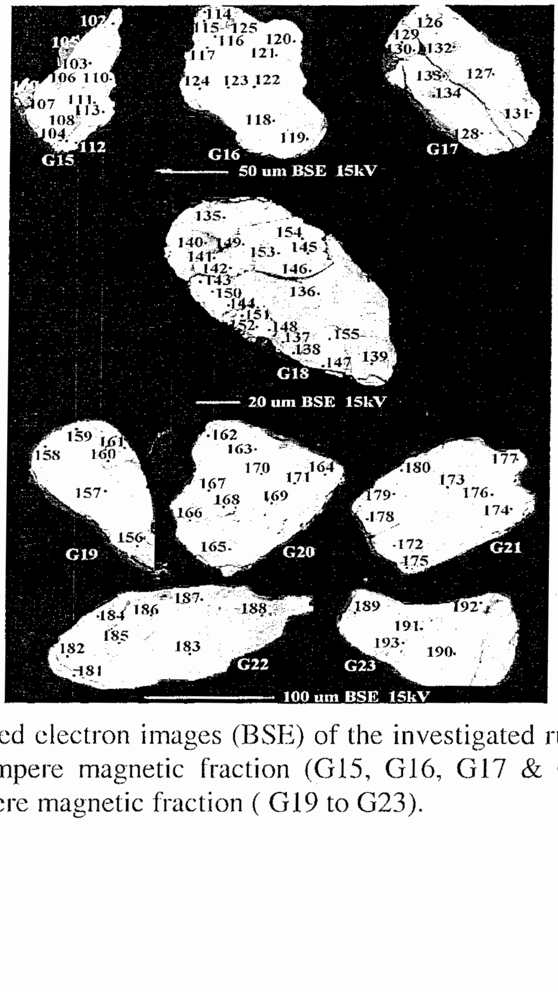

Fig. (6): Back scattered electron images (BSE) of the investigated rutile grains from the obtained 1.5 ampere magnetic fraction (G15, G16, G17 & G18), and from the obtained 3 ampere magnetic fraction (G19 to G23).

The analyzed ilmenite spot (spot 11 in G2), indicates the composition of 53.45% TiO_2, 21.33% FeO and 24.54% MnO. The remaining oxides represent only 0.3%; the total oxides equal 99.62%. The TiO_2 content is almost similar to that characteristic for ilmenite or pyrophanite. Then, the most probable mineralogical composition of the spot is a solid solution between ilmenite ($FeTiO_3$), and pyrophanite ($MnTiO_3$).

Investigating the contents of MnO% in ilmenite-pyrophanite spot (11), leached ilmenite spot (12), and the analyzed pseudorutile spots in G2 and MnO% contents in ilmenite replaced by sphene (spots 20 & 21, Fig.4 and Table 1) may indicate that ilmenite containing relatively high contents of MnO that reflects a relatively high ability for alteration.

In G5, it is obvious that the titanhematite surrounding the pseudobrookite (spot 40) shows a relatively low TiO_2 content than that surrounding the pseudorutile (spot 42, Fig. 4 and Table 1).

Balsley and Buddington (1958) and Boctor (1966) explained that in titanhematite; Fe_2O_3 with 5-10% TiO_2 as $FeTiO_3$ up to about 13% plus excess TiO_2 up to about 3% in solid solution. In fact, some of the analyzed titanhematite spots, in G5 and G6; have TiO_2 contents more than 10%. Therefore, the recorded ferriilmenite lamellae (Spots 68 & 69 in G6, Fig. 4) represent the unmixed excess of $FeTiO_3$ that present originally in solid solution with hematite. Also, the two rutile spots (50&54) in G6 (Fig. 4 and Table 1) may reflect the substitution of TiO_2 by Al_2O_3.

The 0.8 ampere magnetic fraction:

The investigated grains were identified to be composed of rutile (G7, G8, G10 and G12); rutile and titanhematite including ferriferous rutile; spots 81 and 85, (G9); rutile and ilmenite (G11) and finally individual pseudorutile prisms G13&G14 (Fig.5, Table 1).

Table (1): Electron microprobe analyses of the investigated grains from the various magnetic rutile varieties.

Analyses	Na_2O	K_2O	CaO	Al_2O_3	SiO_2	TiO_2	Fe_2O_3	FeO	MnO	MgO	Cr_2O_3	ZnO	ZrO_2	HfO_2	Total	Mineral Component
1	0.00	0.01	0.01	0.00	0.00	98.45	0.67		0.00	0.02	0.08	0.00	0.07	0.02	99.33	Rutile
2	0.02	0.02	0.01	0.06	0.13	99.02	0.52		0.00	0.02	0.01	0.12	0.06	0.05	100.04	Rutile
3	0.00	0.01	0.02	0.50	0.06	97.61	0.58		0.00	0.06	0.00	0.00	0.03	0.10	98.97	Rutile
4	0.02	0.01	0.01	0.00	0.00	99.17	0.55		0.00	0.02	0.02	0.03	0.09	0.12	100.02	Rutile
5	0.01	0.01	0.01	0.00	0.00	99.32	0.55		0.00	0.00	0.03	0.02	0.02	0.07	100.02	Rutile
6	0.00	0.00	0.02	0,00	0.00	99.11	0.62		0.00	0.01	0.06	0.07	0.05	0.06	100.01	Rutile
7	0.00	0.00	0.03	0.00	0.00	99.74	0.46		0.03	0.01	0.00	0.00	0.05	0.07	100.37	Rutile
8	0.03	0.17	0.33	1.20	4.77	63.00	21.36		1.70	0.41	0.13	0.00	0.00	0.06	93.16	Pseudorutile
9	0.03	0.02	0.11	0.04	0.22	61.95	29.27		5.31	0.07	0.03	0.07	0.00	0.04	97.14	Pseudorutile
10	0.09	0.01	0.39	0.55	1.36	69.01	21.61		1.58	0.19	0.13	0.00	0.03	0.08	95.02	Pseudorutile
11	0.01	0.01	0.05	0.00	0.01	53.45		21.33	24.54	0.03	0.00	0.10	0.00	0.09	99.62	Ilmenite+Pyrophanite
12	0.10	0.29	0.31	2.59	9.39	55.68	22.33		2.61	0.95	0.04	0.03	0.02	0.04	94.39	Leached ilmenite
13	0.00	0.01	0.03	0.00	0.00	99.19	0.47		0.00	0.00	0.20	0.00	0.00	0.07	99.97	Rutile
14	0.00	0.00	0.03	0.00	0.00	99.36	0.19		0.00	0.00	0.25	0.02	0.01	0.09	99.95	Rutile
15	0.02	0.00	0.04	0.00	0.00	98.85	0.20		0.02	0.00	0.21	0.00	0.03	0.13	99.50	Rutile
16	0.00	0.01	0.07	0.08	0.17	60.63	35.06		1.01	0.11	0.09	0.00	0.00	0.07	97.30	Pseudorutile
17	0.04	0.01	0.08	0.06	0.18	60.53	35.34		0.93	0.13	0.03	0.00	0.05	0.10	97.48	Pseudorutile
18	0.08	0.00	0.30	0.04	0.22	60.29	33.93		1.05	0.12	0.07	0.03	0.01	0.01	96.15	Pseudorutile
19	0.01	0.02	29.25	0.49	30.55	39.48	0.43		0.03	0.00	0.01	0.00	0.00	0.03	100.29	Sphene
20	0.03	0.02	28.70	0.79	30.48	38.48	1.72		0.04	0.24	0.01	0.19	0.00	0.00	100.70	Sphene
21	0.00	0.01	0.78	0.00	0.00	51.50		38.95	8.20	0.05	0.02	0.00	0.00	0.07	99.56	Ilmenite
22	0.00	0.00	0.76	0.00	0.00	51.85		40.28	7.11	0.01	0.05	0.05	0.01	0.06	100.16	Ilmenite
23	0.00	0.00	0.01	0.00	0.00	99.07	0.47		0.00	0.00	0.09	0.00	0.00	0.10	99.75	Rutile
24	0.00	0.00	0.02	0.00	0.00	98.94	0.38		0.00	0.01	0.07	0.00	0.00	0.06	99.48	Rutile
25	0.04	0.05	0.03	3.50	1.21	91.18	1.28		0.00	0.44	0.10	0.02	0.00	0.09	97.92	Rutile
26	0.05	0.02	0.01	0.58	0.57	97.71	0.73		0.02	0.20	0.20	0.07	0.01	0.09	100.24	Rutile
27	0.00	0.00	0.01	0.00	0.00	99.71	0.56		0.00	0.02	0.10	0.00	0.04	0.10	100.54	Rutile
28	0.03	0.00	0.02	0.00	0.00	99.00	0.91		0.00	0.02	0.16	0.03	0.03	0.06	100.26	Rutile
29	0.01	0.01	0.01	0.00	0.00	98.33	1.42		0.00	0.02	0.14	0.00	0.00	0.11	100.04	Rutile
30	0.00	0.00	0.03	0.00	0.00	98.72	1.43		0.01	0.00	0.10	0.05	0.00	0.07	100.42	Rutile
31	0.02	0.00	0.04	0.00	0.00	98.65	1.22		0.03	0.00	0.13	0.08	0.02	0.06	100.25	Rutile
32	5.71	1.77	0.23	36.45	44.64	1.43	4.74		0.00	1.56	0.26	0.01	0.00	0.00	96.80	Garnet+Feldspar #
33	0.33	0.48	0.35	22.96	35.24	1.54	17.74		0.15	15.36	0.15	0.10	0.03	0.07	94.50	Garnet #
34	0.00	0.01	0.00	0.00	0.00	12.02	88.63		0.00	0.00	0.30	0.19	0.00	0.01	101.15	Titanhematite
35	0.00	0.00	0.00	0.00	0.00	14.80	85.30		0.00	0.00	0.39	0.00	0.01	0.01	100.50	Titanhematite
36	0.00	0.00	0.01	0.00	0.00	11.17	89.43		0.00	0.04	0.29	0.12	0.01	0.00	101.06	Titanhematite
37	0.00	0.01	0.01	0.00	0.00	11.17	88.34		0.00	0.01	0.36	0.00	0.00	0.00	99.90	Titanhematite
38	0.00	0.00	0.02	0.00	0.00	15.53	83.70		0.02	0.00	0.38	0.00	0.04	0.07	99.76	Titanhematite
39	0.00	0.00	0.02	0.00	0.00	8.47	91.18		0.02	0.00	0.36	0.00	0.00	0.00	100.06	Titanhematite
40	0.03	0.01	0.03	0.00	0.00	28.77	70.78		0.00	0.00	0.33	0.13	0.00	0.00	100.08	Pseudobrookite
41	0.01	0.02	0.01	0.11	0.09	14.08	84.71		0.00	0.00	0.32	0.00	0.01	0.02	99.38	Titanhematite
42	0.04	0.02	0.09	0.12	0.11	60.43	36.63		0.00	0.01	0.28	0.00	0.00	0.06	97.80	Pseudorutile
43	0.02	0.00	0.02	0.00	0.00	99.65	0.45		0.00	0.01	0.06	0.00	0.03	0.05	100.29	Rutile
44	0.03	0.01	0.03	0.00	0.00	99.67	0.51		0.02	0.00	0.10	0.10	0.05	0.10	100.60	Rutile
45	0.01	0.00	0.01	0.00	0.00	99.76	0.59		0.01	0.00	0.04	0.09	0.01	0.09	100.61	Rutile
46	0.01	0.00	0.03	0.00	0.00	99.35	0.57		0.02	0.00	0.09	0.00	0.00	0.08	100.15	Rutile
47	0.00	0.00	0.05	3.00	0.07	93.90	0.58		0.00	0.09	0.08	0.09	0.01	0.04	97.91	Rutile
48	0.00	0.00	0.03	0.16	0.07	95.85	0.38		0.03	0.03	0.07	0.00	0.00	0.06	96.67	Rutile
49	0.00	0.00	0.02	0.14	0.08	99.99	0.65		0.00	0.03	0.06	0.00	0.02	0.06	101.06	Rutile
50	0.02	0.02	0.02	3.52	0.04	94.73	0.56		0.03	0.07	0.06	0.00	0.04	0.09	99.19	Rutile
51	0.02	0.00	0.03	0.02	0.03	98.55	0.66		0.00	0.01	0.02	0.03	0.03	0.08	99.47	Rutile

Table (1): Electron microprobe analyses of the investigated grains from the various magnetic rutile varieties.

Analyses	Na_2O	K_2O	CaO	Al_2O_3	SiO_2	TiO_2	Fe_2O_3	FeO	MnO	MgO	Cr_2O_3	ZnO	ZrO_2	HfO_2	Total	Mineral Component
52	0.03	0.01	0.03	0.00	0.00	99.20	1.18		0.00	0.00	0.02	0.00	0.01	0.07	100.54	Rutile
53	0.00	0.01	0.09	0.00	0.00	98.22	2.07		0.00	0.00	0.02	0.00	0.01	0.13	100.55	Rutile
54	0.03	0.02	0.06	7.33	0.24	85.43	0.65		0.00	0.14	0.03	0.00	0.03	0.05	94.00	Rutile
55	0.45	0.10	2.92	3.16	13.02	72.13	5.51		0.08	3.76	0.03	0.04	0.00	0.03	101.22	Rutile+Amphibole #
56	1.62	0.23	9.78	9.73	38.98	14.58	15.47		0.29	10.58	0.04	0.00	0.00	0.00	101.29	Amphibole #
57	0.00	0.02	23.00	23.11	37.63	1.71	13.25		0.30	0.04	0.05	0.04	0.06	0.03	99.22	Garnet #
58	0.02	0.01	22.62	22.63	37.25	1.69	14.96		0.42	0.03	0.00	0.07	0.00	0.02	99.71	Garnet #
59	1.57	0.24	11.68	10.70	45.66	1.40	16.73		0.31	12.73	0.05	0.03	0.00	0.01	101.12	Amphibole #
60	0.07	0.14	0.88	3.03	9.34	43.68	35.64		4.51	2.58	0.01	0.14	0.08	0.03	100.12	Ilmenite+Feldspar #
61	0.02	0.29	1.97	5.13	21.52	31.82	22.84		2.80	7.16	0.01	0.15	0.00	0.05	93.76	Ilmenite+Feldspar #
62	0.00	0.02	0.02	0.00	27.63	14.53	0.13		0.02	0.03	0.05	0.00	55.92	1.75	100.08	Zircon #
63	0.02	0.00	0.01	0.00	0.00	17.43	82.69		0.64	0.04	0.11	0.00	0.03	0.00	100.97	Titanhematite
64	0.00	0.02	0.02	0.00	0.00	9.24	91.12		0.20	0.00	0.11	0.00	0.01	0.02	100.74	Titanhematite
65	0.01	0.02	0.01	0.00	0.00	8.83	92.04		0.10	0.01	0.06	0.00	0.00	0.00	101.08	Titanhematite
66	0.00	0.01	0.02	0.00	0.00	9.74	91.02		0.28	0.01	0.10	0.15	0.00	0.00	101.34	Titanhematite
67	0.01	0.01	0.01	0.00	0.00	8.71	91.52		0.19	0.03	0.09	0.00	0.03	0.00	100.60	Titanhematite
68	0.00	0.00	0.04	0.00	0.00	49.66	47.96		0.33	0.03	0.09	0.03	0.02	0.08	98.23	Ferriilmenite
69	0.02	0.01	0.05	0.00	0.00	50.10	49.17		0.06	0.00	0.09	0.00	0.00	0.06	99.54	Ferriilmenite
70	0.00	0.00	0.01	0.00	0.01	96.49	0.14		0.00	0.00	0.33	0.00	0.32	0.11	97.40	Rutile
71	0.00	0.00	0.02	0.00	0.00	99.53	0.10		0.00	0.00	0.32	0.06	0.32	0.06	100.41	Rutile
72	0.00	0.01	0.00	0.00	0.00	99.80	0.05		0.00	0.01	0.30	0.01	0.29	0.08	100.55	Rutile
73	0.00	0.00	0.01	0.11	0.00	100.17	0.18		0.00	0.01	0.34	0.00	0.25	0.08	101.14	Rutile
74	0.00	0.00	0.01	0.00	0.00	99.11	0.03		0.00	0.01	0.18	0.04	0.09	0.05	99.51	Rutile
75	0.00	0.02	0.01	0.00	0.00	99.76	0.02		0.02	0.00	0.12	0.00	0.03	0.03	100.00	Rutile
76	0.01	0.02	0.01	0.00	99.89	0.85	0.00		0.00	0.00	0.03	0.00	0.00	0.02	100.82	Silicon dioxide #
77	0.00	0.00	0.00	0.00	99.31	0.90	0.00		0.00	0.01	0.00	0.00	0.00	0.02	100.23	Silicon dioxide #
78	0.00	0.00	0.03	0.00	0.00	99.54	0.46		0.00	0.00	0.02	0.02	0.01	0.07	100.15	Rutile
79	0.00	0.00	0.01	0.00	0.00	99.07	0.55		0.01	0.03	0.03	0.00	0.03	0.03	99.75	Rutile
80	0.00	0.01	0.13	0.00	0.00	98.87	1.42		0.00	0.00	0.05	0.00	0.06	0.07	100.61	Rutile
81	0.00	0.02	0.01	0.00	0.00	79.63	19.15		0.00	0.03	0.02	0.03	0.00	0.11	98.99	Ferriferous Rutile
82	0.00	0.00	0.00	0.05	0.00	6.90	93.29		0.07	0.01	0.06	0.02	0.00	0.04	100.43	Titanhematite
83	0.00	0.00	0.01	0.01	0.00	6.41	93.00		0.06	0.04	0.04	0.00	0.04	0.01	99.63	Titanhematite
84	0.03	0.00	0.02	0.04	0.00	5.00	94.21		0.07	0.08	0.05	0.02	0.05	0.03	99.60	Titanhematite
85	0.06	0.00	0.01	0.01	0.00	79.10	19.48		0.00	0.00	0.05	0.00	0.01	0.02	98.74	Ferriferous Rutile
86	0.03	0.00	0.01	0.00	0.02	99.40	0.22		0.00	0.00	0.16	0.00	0.11	0.07	100.01	Rutile
87	0.01	0.00	0.01	0.00	0.00	99.42	0.14		0.02	0.00	0.19	0.01	0.10	0.05	99.93	Rutile
88	0.05	0.27	0.37	5.70	10.20	73.35	4.36		0.00	0.96	0.10	0.10	0.05	0.00	95.50	Rutile+Garnet #
89	0.00	0.00	0.01	0.00	0.00	99.18	0.29		0.00	0.00	0.12	0.02	0.12	0.09	99.82	Rutile
90	0.00	0.00	0.00	0.00	0.00	99.52	0.16		0.00	0.00	0.18	0.00	0.12	0.08	100.06	Rutile
91	0.00	0.00	0.01	0.00	0.00	53.42		45.30	0.18	0.21	0.05	0.21	0.00	0.02	99.39	Ilmenite
92	0.00	0.02	0.02	0.00	0.00	53.15		45.59	0.11	0.24	0.00	0.04	0.00	0.04	99.21	Ilmenite
93	0.00	0.00	0.01	0.00	0.00	53.92		44.12	0.16	0.24	0.04	0.15	0.02	0.07	98.73	Ilmenite
94	0.00	0.00	0.02	0.00	0.00	68.50		30.28	0.06	0.17	0.10	0.13	0.00	0.08	99.34	Ilmenite
95	0.14	9.55	0.08	21.88	37.28	3.27	13.58		0.00	10.75	0.36	0.05	0.00	0.03	96.95	Mica #
96	0.02	0.00	0.02	0.00	0.00	98.63	0.12		0.00	0.01	0.24	0.02	0.29	0.08	99.44	Rutile
97	0.00	0.00	0.00	0.00	0.00	98.53	0.04		0.00	0.00	0.25	0.00	0.32	0.04	99.18	Rutile
98	0.09	0.05	0.06	1.65	0.00	65.01	22.95		0.03	6.80	0.96	0.03	0.16	0.02	97.81	Pseudorutile
99	0.16	0.01	0.08	1.72	0.04	63.24	24.83		0.08	7.23	0.88	0.00	0.14	0.06	98.45	Pseudorutile
100	0.00	0.01	0.03	1.25	0.02	61.68	28.15		0.13	6.59	0.48	0.11	0.18	0.04	98.66	Pseudorutile
101	0.01	0.00	0.02	1.32	0.01	61.74	28.64		0.12	6.51	0.48	0.12	0.17	0.11	99.24	Pseudorutile
102	0.00	0.01	0.04	0.00	0.00	99.41	0.34		0.00	0.00	0.07	0.01	0.01	0.05	99.93	Rutile
103	0.00	0.00	0.01	0.00	0.00	98.99	0.37		0.01	0.00	0.09	0.08	0.00	0.08	99.63	Rutile
104	0.02	0.00	0.01	0.00	0.00	97.66	2.09		0.00	0.01	0.05	0.02	0.00	0.06	99.92	Rutile
105	9.11	0.07	5.32	23.65	62.13	1.00	0.01		0.00	0.00	0.00	0.00	0.00	0.00	101.26	Feldspar #

Table (1): Electron microprobe analyses of the investigated grains from the various magnetic rutile varieties.

Analyses	Na_2O	K_2O	CaO	Al_2O_3	SiO_2	TiO_2	Fe_2O_3	FeO	MnO	MgO	Cr_2O_3	ZnO	ZrO_2	HfO_2	Total	Mineral Component
106	0.00	0.00	0.00	0.00	97.68	3.15	0.03		0.00	0.00	0.01	0.04	0.03	0.00	100.95	Silicon dioxide #
107	0.00	0.00	0.02	0.00	99.96	0.46	0.14		0.00	0.01	0.01	0.15	0.00	0.00	100.74	Silicon dioxide #
108	0.02	0.01	0.01	0.00	99.47	0.61	0.94		0.01	0.00	0.00	0.08	0.00	0.01	101.17	Silicon dioxide #
109	0.01	0.00	23.27	23.20	36.71	0.49	13.29		0.17	0.03	0.04	0.00	0.05	0.02	97.29	Garnet #
110	0.04	0.00	0.04	0.35	0.17	12.80	86.40		0.27	0.07	0.18	0.07	0.00	0.02	100.40	Titanhematite
111	0.00	0.01	0.00	0.00	0.00	13.15	85.89		0.31	0.08	0.21	0.02	0.00	0.02	99.68	Titanhematite
112	0.03	0.00	0.01	0.00	0.00	8.71	89.28		0.00	0.03	0.29	0.07	0.00	0.03	98.45	Titanhematite
113	0.03	0.00	0.01	0.00	0.00	49.25	48.87		0.05	0.00	0.23	0.01	0.03	0.05	98.52	Ferriilmenite
114	0.01	0.00	0.00	0.00	0.00	98.41	0.56		0.00	0.02	0.04	0.11	0.01	0.03	99.18	Rutile
115	0.00	0.00	0.02	0.00	0.00	98.74	0.56		0.00	0.00	0.00	0.06	0.03	0.05	99.46	Rutile
116	0.00	0.02	0.02	0.11	0.02	99.92	0.59		0.00	0.00	0.05	0.01	0.02	0.10	100.84	Rutile
117	0.04	0.01	0.02	0.00	0.00	99.55	0.51		0.02	0.00	0.00	0.02	0.03	0.08	100.26	Rutile
118	0.03	0.00	0.01	0.00	0.00	99.55	0.46		0.00	0.00	0.01	0.07	0.02	0.03	100.19	Rutile
119	0.01	0.01	0.02	0.00	0.00	99.10	0.42		0.00	0.00	0.00	0.07	0.05	0.11	99.79	Rutile
120	0.02	0.01	0.22	0.35	0.57	66.05	25.08		1.60	0.20	0.14	0.14	0.00	0.07	94.46	Pseudorutile
121	0.00	0.03	0.18	0.32	0.56	67.85	25.46		1.34	0.25	0.11	0.11	0.06	0.09	96.34	Pseudorutile
122	0.07	0.03	0.15	0.36	0.63	65.36	26.29		1.36	0.28	0.12	0.20	0.14	0.10	95.07	Pseudorutile
123	0.07	0.01	0.24	0.27	0.49	68.61	24.49		1.35	0.20	0.07	0.04	0.68	0.00	96.51	Pseudorutile
124	0.06	0.03	0.22	0.36	0.66	67.01	25.16		1.27	0.22	0.14	0.00	0.07	0.11	95.30	Pseudorutile
125	0.11	2.35	0.41	25.68	49.79	1.57	8.83		0.03	3.21	0.04	0.10	0.04	0.00	92.15	Garnet+Feldspar #
126	0.00	0.00	0.03	0.00	0.01	98.60	0.35		0.01	0.00	0.13	0.01	0.04	0.08	99.26	Rutile
127	0.03	0.01	0.01	0.00	0.00	99.12	0.37		0.00	0.00	0.09	0.01	0.02	0.06	99.72	Rutile
128	0.00	0.01	0.01	0.00	0.00	100.03	0.31		0.00	0.01	0.06	0.10	0.00	0.05	100.59	Rutile
129	0.01	0.01	0.02	0.00	0.00	53.62		43.13	1.24	1.09	0.05	0.13	0.00	0.05	99.34	Ilmenite
130	0.00	0.01	0.02	0.06	0.02	58.64	40.11		0.96	0.45	0.04	0.07	0.00	0.04	100.42	Leached ilmenite
131	0.02	0.01	0.01	0.00	0.00	53.72		43.09	1.15	1.02	0.02	0.14	0.03	0.02	99.23	Ilmenite
132	2.04	0.15	11.55	14.52	43.64	1.97	12.56		0.17	12.51	0.03	0.07	0.00	0.00	99.20	Garnet+Feldspar #
133	0.01	0.00	23.86	26.73	37.86	1.57	8.32		0.12	0.01	0.09	0.04	0.00	0.00	98.60	Garnet #
134	0.03	0.00	17.76	22.91	38.43	2.00	9.00		0.14	6.29	0.08	0.02	0.00	0.05	96.70	Garnet #
135	0.00	0.01	0.02	0.00	0.00	98.47	0.42		0.00	0.00	0.00	0.05	0.00	0.12	99.09	Rutile
136	0.00	0.00	0.02	0.00	0.00	99.03	0.48		0.03	0.00	0.05	0.01	0.05	0.04	99.70	Rutile
137	0.01	0.03	0.05	0.84	1.87	93.22	0.90		0.03	0.17	0.01	0.02	0.04	0.13	97.31	Rutile
138	0.00	0.01	0.03	0.06	0.02	97.92	0.40		0.03	0.01	0.06	0.00	0.02	0.10	98.65	Rutile
139	0.01	0.00	0.01	0.00	0.00	99.38	0.42		0.03	0.01	0.03	0.08	0.00	0.08	100.04	Rutile
140	0.01	0.02	0.02	0.25	0.00	100.03	0.61		0.00	0.03	0.06	0.11	0.00	0.09	101.22	Rutile
141	0.02	0.01	0.08	0.00	0.08	60.85	33.56		1.11	0.26	0.03	0.03	0.00	0.00	96.04	Pseudorutile
142	0.03	0.01	0.05	0.00	0.08	60.19	34.42		1.10	0.29	0.05	0.18	0.00	0.10	96.49	Pseudorutile
143	0.03	0.00	0.11	0.00	0.05	61.35	33.52		0.99	0.29	0.01	0.00	0.03	0.03	96.42	Pseudorutile
144	0.03	0.02	0.09	0.28	0.18	60.66	31.59		1.13	0.22	0.05	0.04	0.00	0.00	94.30	Pseudorutile
145	0.00	0.00	0.10	0.00	0.06	61.20	33.53		0.98	0.34	0.06	0.00	0.00	0.08	96.36	Pseudorutile
146	0.00	0.01	0.04	0.00	0.06	60.26	34.57		1.14	0.35	0.03	0.06	0.00	0.10	96.62	Pseudorutile
147	0.00	0.00	0.05	0.01	0.02	59.22	34.61		1.23	0.19	0.00	0.00	0.00	0.03	95.36	Pseudorutile
148	0.00	0.00	0.16	0.04	0.08	65.15	28.99		0.96	0.22	0.01	0.04	0.00	0.04	95.69	Pseudorutile
149	0.12	0.03	0.45	0.54	0.93	71.97	19.31		0.17	0.19	0.17	0.04	0.13	0.05	94.11	Leached Pseudorutile
150	0.13	0.04	0.51	0.53	0.91	71.57	20.02		0.17	0.19	0.17	0.09	0.02	0.02	94.36	Leached Pseudorutile
151	0.09	0.05	0.50	0.54	0.81	70.19	20.36		0.31	0.19	0.15	0.07	0.06	0.05	93.37	Leached Pseudorutile
152	0.08	0.00	0.46	0.50	0.82	70.83	20.03		0.27	0.23	0.16	0.12	0.08	0.00	93.56	Leached Pseudorutile
153	0.12	0.02	0.47	0.52	0.90	71.31	19.79		0.22	0.24	0.17	0.02	0.07	0.06	93.90	Leached Pseudorutile
154	0.09	0.01	0.43	0.44	0.72	69.42	21.91		0.37	0.27	0.20	0.04	0.07	0.01	93.98	Leached Pseudorutile
155	0.13	0.02	0.53	0.48	0.79	70.43	19.32		0.12	0.20	0.24	0.04	0.00	0.05	92.34	Leached Pseudorutile
156	0.00	0.00	0.02	0.00	0.00	98.96	0.12		0.00	0.02	0.11	0.03	0.18	0.11	99.54	Rutile
157	0.00	0.01	0.00	0.00	0.00	99.76	0.18		0.00	0.00	0.04	0.00	0.17	0.08	100.23	Rutile
158	0.01	0.00	0.07	0.09	0.11	61.23	33.31		0.25	0.34	0.00	0.00	0.01	0.02	95.44	Pseudorutile
159	0.02	0.03	0.10	0.21	0.33	62.98	31.27		0.08	0.26	0.02	0.00	0.03	0.05	95.39	Pseudorutile
160	0.00	0.03	0.05	0.59	1.00	62.31	33.41		0.04	0.68	0.03	0.00	0.06	0.06	98.25	Pseudorutile

MINERALOGICAL CHARACTERISTICS OF THE SEPARATED

Table (1): Electron microprobe analyses of the investigated grains from the various magnetic rutile varieties.

Analyses	Na_2O	K_2O	CaO	Al_2O_3	SiO_2	TiO_2	Fe_2O_3	FeO	MnO	MgO	Cr_2O_3	ZnO	ZrO_2	HfO_2	Total	Mineral Component
161	0.01	0.00	0.03	0.09	0.18	62.12	33.96		0.35	0.77	0.06	0.01	0.01	0.07	97.65	Pseudorutile
162	0.01	0.00	0.00	0.00	0.00	99.48	0.50		0.00	0.00	0.04	0.00	0.00	0.04	100.07	Rutile
163	0.01	0.00	0.00	0.00	0.00	99.65	0.48		0.02	0.00	0.02	0.01	0.00	0.11	100.30	Rutile
164	0.02	0.00	0.01	0.00	0.00	99.69	0.42		0.00	0.00	0.04	0.00	0.03	0.12	100.32	Rutile
165	0.03	0.00	0.01	0.00	0.00	99.98	0.43		0.00	0.00	0.05	0.00	0.00	0.10	100.58	Rutile
166	0.00	0.00	0.02	0.00	0.00	98.95	0.60		0.04	0.01	0.07	0.00	0.06	0.12	99.86	Rutile
167	0.01	0.01	0.07	0.00	0.11	69.77	23.12		0.18	0.21	0.01	0.07	0.00	0.07	93.63	Pseudorutile
168	0.05	0.02	0.10	0.06	0.18	63.36	32.40		0.58	0.21	0.03	0.05	0.02	0.07	97.12	Pseudorutile
169	0.02	0.00	0.08	0.04	0.09	63.24	31.10		0.90	0.23	0.04	0.05	0.00	0.03	95.82	Pseudorutile
170	0.01	0.02	0.01	0.00	0.00	54.04		39.65	3.50	0.16	0.04	0.03	0.00	0.02	97.48	Ilmenite
171	0.01	0.01	0.02	0.00	0.00	52.09		42.67	4.21	0.19	0.07	0.05	0.00	0.05	99.36	Ilmenite
172	0.01	0.00	0.01	0.00	0.00	99.33	0.41		0.02	0.01	0.09	0.06	0.01	0.07	100.00	Rutile
173	0.01	0.01	0.00	0.00	0.00	99.49	0.46		0.00	0.01	0.05	0.00	0.10	0.05	100.18	Rutile
174	0.00	0.01	0.01	0.00	0.00	99.04	0.37		0.03	0.00	0.02	0.00	0.02	0.03	99.52	Rutile
175	0.01	0.03	0.07	0.09	0.33	53.21		41.69	1.38	0.04	0.00	0.15	0.00	0.03	97.01	Ilmenite
176	0.03	0.00	0.00	0.00	0.00	53.75		44.70	1.15	0.03	0.02	0.05	0.00	0.00	99.73	Ilmenite
177	0.00	0.00	0.01	0.00	0.00	52.31		44.94	1.35	0.02	0.04	0.10	0.00	0.09	98.85	Ilmenite
178	0.02	0.00	0.00	0.00	0.00	52.55		45.07	1.29	0.03	0.00	0.04	0.00	0.03	99.03	Ilmenite
179	0.03	0.02	0.01	0.00	0.00	53.64		44.08	1.19	0.01	0.02	0.05	0.03	0.06	99.13	Ilmenite
180	0.00	0.00	0.01	0.00	0.00	57.99	41.38		1.07	0.01	0.00	0.00	0.00	0.00	100.47	Leached ilmenite
181	0.00	0.01	0.03	0.00	0.00	98.26	0.07		0.01	0.01	0.01	0.07	0.01	0.10	98.55	Rutile
182	0.00	0.00	0.02	0.00	0.00	98.89	0.01		0.00	0.03	0.09	0.02	0.07	0.07	99.20	Rutile
183	0.02	0.00	0.00	0.00	0.00	99.08	0.01		0.00	0.00	0.05	0.06	0.06	0.09	99.37	Rutile
184	0.09	0.01	0.53	0.75	1.02	76.43	13.99		0.30	0.22	0.08	0.29	0.00	0.03	93.75	Leached Pseudorutile
185	0.05	0.05	0.42	0.64	0.87	74.21	15.29		0.52	0.22	0.03	0.16	0.02	0.11	92.58	Leached Pseudorutile
186	0.11	0.01	0.53	0.74	0.97	75.97	13.79		0.30	0.22	0.03	0.23	0.06	0.06	93.02	Leached Pseudorutile
187	0.10	0.01	0.51	0.79	0.97	76.23	14.02		0.34	0.21	0.05	0.25	0.06	0.07	93.61	Leached Pseudorutile
188	0.09	0.00	0.53	0.73	0.98	76.04	14.39		0.21	0.19	0.00	0.24	0.01	0.09	93.49	Leached Pseudorutile
189	0.01	0.00	0.01	0.00	0.00	99.36	0.49		0.00	0.00	0.05	0.00	0.08	0.13	100.13	Rutile
190	0.01	0.01	0.00	0.00	0.00	99.56	0.47		0.00	0.03	0.07	0.08	0.04	0.00	100.26	Rutile
191	0.02	0.02	0.05	0.03	0.07	58.47	36.79		2.59	0.06	0.05	0.00	0.03	0.07	98.25	Leached ilmenite
192	0.04	0.09	0.18	0.92	2.72	60.08	28.97		1.75	0.28	0.13	0.14	0.01	0.08	95.38	Pseudorutile
193	0.02	0.02	0.12	0.91	1.25	77.31	15.47		1.37	0.10	0.18	0.00	0.07	0.07	96.88	Leached Pseudorutile

 # The identified inclusions.

Table (2): The investigated grains and the analyzed spots of the different identified mineral components and inclusions in the various magnetic rutile farctions.

The used current ampere	Description of grains	The investigated grains and analyzed spots	The number of identified inclusions	The identified mineral components*	The type of identified inclusions
0.4	Dark red, red, orange and/or yellow rutile included, coated, stained or composited with opaque zones	(G1 to G6) From spot 1 to spot 69	10	Rutile,titanhematite, pseudorutile, ferriilmeinte and pseudobrookite.	Garnet, amphibole ilmenite, feldspar, zircon
0.8	Dark red, red, orange and/or yellow rutile included, coated, stained or composited with opaque zones	(G7 to G11) From spot 70 to spot 95	4	Rutile, ilmenite, titanhematite and ferriferous rutile.	Silicon dioxide, garnet, mica
0.8	Euhedral-subhedral dark red prismatic crystals with relatively high elongation ratio.	(G12 to G14) From spot 96 to spot 101	-	Rutile, individual pseudorutile	-
1.5	Dark red, red, orange and/or yellow rutile included, coated, stained or composited with opaque zones	(G15 to G18) From spot 102 to spot 155	9	Rutile, pseudorutile, leached pseudorutile,titanhematite, ilmenite	Silicon dioxide, garnet, feldspar
3.0	Dark red, red, orange and/or yellow rutile included, coated, stained or composited with opaque zones	(G19 to G23) From spot 156 to spot 193	-	Rutile, pseudorutile, leached pseudorutile, ilmenite	-

*** The mineral components are arranged in a decreasing order of abundance for each magnetic fraction.**

The magnetic characters of the detected rutile grains that seem to be homogenous and composed completely of rutile are due to one or more of the following reasons:

a- Magnetic inclusions of micronized sizes.

b- Inclusions in definite crystallographic orientations other than that of the detected polished area.

c- The deviation from the 1 : 2 (Ti : O) stoichiometry in synthetic rutiles, grown or heated under reducing conditions or doped with various impurities that give rise to a variety of interesting optical and electronic properties that have been extensively studied (Strawmanis et al., 1961; Johnson et al. 1968; and Khomenko et al. 1998). Such deviation in Ti : O ratio my be also affects the magnetic characters of these rutiles.

On the other hand, the two detected prismatic crystals of individual pseudorutile (G13 & G14) seem to be of primary origin. They have characteristic chemical contents where Al_2O_3 are 1.25 and 1.72%, MgO are 6.51 and 7.23%, and Cr_2O_3 are 0.48 and 0.96%, respectively. Also, relatively greater sum total oxide contents (97.81 and 99.24%) in addition to the euhedral -subhedral crystal habits.

The 1.5 ampere magnetic fraction:

The identified grains were composed of rutile and titanhematite that including exsolved ilmenite lamellae (G15), rutile and pseudorutile (G16); rutile and ilmenite (G17), and rutile, pseudorutile and leached pseudorutile; G18 (Fig. 6 & Tables 1,2). In these cases, the analyzed spots of pseudorutile seem to be of secondary origin after ilmenite. The reason is the relatively lower sum of total oxides and the characteristic MnO contents which are similar to those detected within the analyzed spots of the associated identified ilmenite (spots 129&131 in G 17, Fig. 6).

According to Temple (1966), the oxidation and partial removal of iron from ilmenite lattice results in the formation of pseudorutile which contains (65-70%) TiO_2 at the complete oxidation stage of the original iron in the ilmenite.

Gevorkyan and Tananayev (1964), explained that within the pseudorutile composition range (60-71% TiO_2), the water content increased from ~ 2 to 4.5 wt.% with decreasing iron oxide content. They proposed that the intermediate alteration phases comprise mixtures of TiO_2 with iron hydroxides. On the other hand, Gery et al. (1994) stated that pseudorutile $Fe_2^{3+}Ti_3O_9$ has recently been revalidated as a mineral species with a hexagonal primitive unit cell. It is formed due to the alteration of ilmenite by the removal of Fe^{2+}. The electrostatic charge balance is maintained by oxidation of the remaining iron to Fe^{3+} and/or the addition of H^+. If the Fe^{2+} is removed in any regular pattern, then the pseudorutile will show ordering.

Frost et al., (1983), explained that pseudorutile may be an oxyhydroxide mineral with an extended range of homogeneity due to replacement of Fe^{3+} by $3H^+$ giving the general formula $Fe^{3+}_{2-x}Ti_3O_{9-3x}$ $(OH)_{3x}$. Chernet (1999) and Chernet and Pakkanen (2003), identified the alteration product, which deviates substantially from the ideal ilmenite composition but not completely altered to pseudorutile, as leached ilmenite. Further alteration of pseudorutile to leucoxene often shows an intermediate product identified as leached pseudorutile. Along with the advance of the alteration, the water content increases until the breakdown of a pseudorutile structure, which appears at the composition of about (77 – 79%) TiO_2 and (9-12%) Fe_2O_3; the remaining percentage is mostly H_2O molecules (Chernet, 1999).

In fact, all the analyzed spots of pseudorutile and leached pseudorutile are in agreement with most of the forementioned published results. The depletion of the sum of the total oxides (from 92.34-94.36 % for spots 149-155, G18), is due to the presence of water molecules which are corresponding to the added hydroxyl ions due to ilmenite alteration into pseudorutile and/or leached pseudorutile. The contents of MnO% in ilmenite and leached ilmenite in G17 and for pseudorutile and leached pseudorutile in G18 (see Fig. 6 and Table 1) may indicate the high alteration ability of ilmenite containing relatively high contents of MnO.

Also, the analyzed leached pseudorutile spots; 149 to 155, in G18 (Fig. 6 and Table 1), may reflect the role of SiO_2, Al_2O_3 and/or CaO in the process of ilmenite alteration.

The 3 ampere magnetic fraction:

The identified grains were composed of rutile and pseudorutile (G19); rutile and pseudorutile with relics of preexisting ilmenite (G20); rutile and ilmenite (G21); rutile and leached pseudorutile (G22) in addition to rutile with leached ilmenite, leached pseudorutile and ilmenite; G23 (Fig. 6, Tables 1,2).

In these cases, the pseudoruitle and leached pseudorutile are considered to be secondary in origin due to the alteration of preexisting ilmenite. Also, their chemical analyses are confirmed with the concepts of Chernet (1999) and Chernet and Pakkanen (2003). The contents of MnO% for ilmenite and leached ilmenite in

G21 and for leached ilmenite, pseudorutile and leached pseudorutile in G23 (see Fig. 6 and Table 1) may ensure that ilmenite containing relatively high contents of MnO has relatively high ability for alteration into leached ilmenite, pseudorutile followed by leached pseudorutile, which has the lowest MnO% content.

It was noticed that for only the intermediate alteration product defined as leached pseudorutile (spots 184-188 in G22, Fig. 6 and Table 1), the contents of SiO_2, Al_2O_3 and/or CaO are relatively high. This may reflect the role of one or more of these oxides in the later stages of pseudorutile alteration to give the relatively enriched TiO_2 alteration products.

3.2 The identified inclusions

Several inclusions were detected in the various rutile grains. They include garnet, silicon dioxide, amphibole, ilmenite, feldspar, mica and zircon. These inclusions reflect the derivation of the studied magnetic rutile from different crystalline igneous and metamorphic rocks.

3.3 The magnetic characters of the studied rutile varieties.

Concerning with the mass magnetic susceptibilities of the various investigated rutile varieties, it can be concluded that both of the associated mineral component species and their corresponding sizes in relation to the associated rutile mineral component, govern the magnetic behaviour of these grains. The type and size of the associated inclusions are also considered another important factor affecting the magnetic behaviour of the grains. It is obvious that the rutile grains contain relatively high content of titanhematite, that may contain considerable contents of dissolved TiO_2 and definite inclusion species of ilmenite, garnet and/or amphibole (G5 & G6, Fig. 4), have relatively high mass magnetic susceptibilities. It is clear that rutile grains containing for small parts of ilmenite (G11, Fig. 5), or have titanhematite of relatively lower dissolved TiO_2 contents (G9, Fig. 5), and do not contain appreciable parts of magnetic inclusions, have moderate magnetic characters as the identified individual pseudorutile grains (G 13 & G14, Fig. 5).

The grains containing for relatively low contents of titanhematite (G15, Fig. 6), or ilmenite (G 17, Fig. 6), and/or relatively low contents of pseudorutile (G16 & G18, Fig. 6), have weak magnetic characters. On the other hand, the grains of much low contents of pseudorutile, ilmenite and/or contain only leached pseudorutile (G19, G20, G21, G22 & G23, Fig. 6), have the lowest magnetic characters.

3.4 The quality of the Egyptian beach high–grade rutile concentrate.

The high grade rutile concentrate contains more than 97% TiO_2 and most of the other analyzed minor oxides are within the accepted limits of marketable specification (Hammoud 1966 & 1973 and Moustafa, 1999). Neglecting the identified mineral inclusions in the studied magnetic rutile varieties and calculating the average chemical composition of the other analyzed spots, the following contents are obtained: TiO_2, 66.34%, Fe_2O_3, 21.71%; SiO_2, 6.39%; Al_2O_3, 1.8%; CaO, 1.19% and Cr_2O_3, 0.10%. Then, if the magnetic rutile varieties are included within the high – grade rutile concentrate, it may affect the marketable specification of the concentrate. It is recommended to blend these magnetic rutile varieties with magnetic leucoxene or with definite amounts of some types of the Egyptain ilmenite concentrates to improve the marketable specification especially for Ti, Fe and Cr.

CONCLUSIONS

During the concentration and separation of the Egyptian beach high-grade rutile concentrate, some magnetic rutile varieties are contained in the final obtained magnetic fractions. These varieties represent about 4% of the original rutile content in the raw sands.

The identification of the different magnetic rutile varieties; using electron microprobe analyses revealed the following mineral components in a decreasing order of abundance: rutile, titanhematite, pseudorutile, leached pseudorutile and ilmenite in addition to the existance of individual pseudorutile crystals which are most probably of primary origin.

It was concluded that the ilmenite which contains high MnO contents has more ability for alteration into other mineral components characterized by relatively low MnO contents.

Both of SiO_2, Al_2O_3 and/or CaO may play important roles in ilmenite alteration process, especially in the final stages of alteration (e.g. leached pseudorutile).

Several mineral inclusions are detected; they are composed most probably of garnet, silicon dioxide, amphibole, ilmenite, feldspar, mica and zircon. The identified inclusions may reflect the derivation of the magnetic rutile varieties from various crystalline igneous and metamorphic rocks.

MINERALOGICAL CHARACTERISTICS OF THE SEPARATED

The mass magnetic susceptibilities of the different magnetic rutile varieties are governed by the types and amount of the associated mineral components, in addition to the type and size of contained inclusions.

It is difficult to liberate the different mineral components; and inclusions, associsted with rutile using grinding followed by various ore dressing techniques. Then, the removal of these magnetic rutile mineral varieties improve the quality of the obtained high-grade rutile concentrate. These varieties can be blended with definite amounts of magnetic leucoxene or some types of ilmenite concentrates to improve their marketable specifications especially for Ti, Fe, and Cr.

Acknowledgement

The author wish to thank Prof. Dr. H.J. Massonne, Dr. Thomas Theye and the microprobe Laboratory Group of Institute of Mineralogy and Crystal Chemistry, Stuttgart University, Germany, for their efforts during the analytical work.

REFERENCES

Balsley, J.R. and Buddington, A.F. (1958): Iron-titanium oxide minerals, rocks, and aeromagnetic anomalies of the Adirondack area, New York. Econ. Geol., Vol.53, No.7, pp.777-805.

Bishady, A.M.; Dawoud, M.; Khazbak, A.E.; Saad, and El Nahas, H. (2004): Mineralogy, evaluation and upgrading of the titanium bearing minerals from beach black sands of El Kharouba area, Sinai, Egypt. The seventh international conference on the geology of the Arab World (GAW-7), Geol. Dept., Fac. Sci., Cairo Univ., Egypt, pp.81-90.

Boctor, N.Z. (1966): Mineralogical study of the opaque minerals in Rosetta-Damietta black sands. M.Sc. Thesis, Fac. Sci., Cairo Univ., Egypt.

Cherent, T. (1999): Applied mineralogical studies on Australian sand ilmenite concentrate with special reference to their behaviour in sulphate route pigment extraction process. International Journal of Minerals Engineering, 12(5), pp. 485 – 495.

Chernet, T. and Pakkanen, L. (2003): Estimation of ferric iron, crystal water and calculation of chemical formulae for altered ilmenite from electron microprobe analyses, based on stoichiometric criteria. Geological survey of Finland, Special paper 36, pp. 23-28.

Dabbour, G.A. (1980): Geological and mineralogical studies on rutile in the black sands deposits from the Egyptian Mediterranean Coast. Ph.D.Thesis, Fac. Sci., Cairo Univ., Egypt.

Dabbour, G.A. (1997): Mineralogical study on the opaque minerals and secondary rutile from the Egyptian black sands. Proceed. Egypt. Acad. Sci., Vol.47, pp.105-121.

Dewedar, A.A.M. (1998): Comparative studies on the heavy minerals in some black sand deposits from Sinai and east Rosetta, with contributions to the mineralogy and economics of their garnets. Ph.D. Thesis, Fac. Sci., Menoufia Univ., Egypt.

El Hinnawi, E.E. (1964): Minerlogical and geochemical studies on Egyptian (U.A.R.) black sands. Beitrage zur Mineralogie and Petrologie, Vol.9, pp.519-532.

Frost, M.T.; Grey, I.E.; Harrowfield, I.R. and Mason, K. (1983): The dependence of alumina and silica contents on the extent on alteration of weathered ilmenites from western Australia. Miner. Mag., Vol.47, June, pp.201-208.

Gevorkyan, V. kh. And Tananayev, N.V. (1964): Some data on the initial stages of leucoxenization of ilmenite from the sedimentary deposits of the northern Azov area. Dopovidi Akademi Nauk Ukrains Koi RSR, 10, pp. 1366 – 1369.

Grey, I.E.; Watts, J.A. and Bayliss, P. (1994): Mineralogical nomenclature: Pseudorutile revalidated and neotype given. Mineral. Mag., Vol.58, December, pp.597-600.

Hammoud, N. M. (1966): Concentration of monazite from Egyptian black sands, employing industrial techniques. M.Sc. Thesis, Fac. Sci., Cairo Univ., Egypt.

Hammoud, N. M. (1973): Physical and chemical properties of some Egyptian beach economic minerals in relation to their concentration problems. Ph.D. Thesis, Fac. Sci., Cairo Univ., Egypt.

Johnson, O.W.; Olsen, W.D. and Kingsbury, P.I. (1968): Defects in rutile. III. Optical and electrical properties of impurities and charge carriers. Phys. Rev., 175, pp. 1102 – 1109.

Kamel, K.E. (1964): Mineralogical and petrographical studies on the transparent economic minerals of the black sands of Rosetta, Egypt. M.Sc. Thesis, Fac. Sci., Assiut Univ., Egypt.

Khomenko, V.M., Langer, K., Rager, H. and Fett, A. (1998): Electronic absorption by Ti^{3+} ions and electron delocalization in synthetic blue rutile. Phys. Chem.. Minerals, 25, pp. 338 - 346.

Mikhail, M.A. (1971): Distribution and sedimentation of ilmenite in black sands, west of Rosetta. M.Sc. Thesis, Fac. Sci., Cairo Univ., Egypt.

Mohamed, E.H. (1987): Mineralogical studies for some Quaternary sediments in northern Sinai. M.Sc. Thesis, Fac. Sci., Suez Canal Univ., Ismailia, Egypt.

Moustafa, M. I. (1995): Investigations of some physical properties of zircon and rutile to prepare high purity mineral concentrates from black sand deposits, Rosetta, Egypt. M.Sc. Thesis, Fac. Sci., Mansoura Univ., Egypt.

Moustafa, M. I. (1999): Mineralogy and beneficiation of some economic minerals in the Egyptian black sands. Ph.D. Thesis, Fac. Sci., Mansoura University, Egypt.

Moustafa, M. I. (2003): Separation of economic minerals and discovery of zinc, lead and mercury minerals in the Egyptian black sands, the third international conference of the geology of Africa, Geol. Dept., Fac., Scie., Assuit Univ., Egypt, 153-171.

Moustafa, M. I. (2007): Geochemical studies of the Egyptian beach cassiterite concentrate and its importance as a source of Sn, Ta, Nb and others. The fifth international conference on the geology of Africa, Fac. Sci., Assiut Univ., 1, 63-78, Assiut, Egypt.

Naim, G.M.; El Miligy, A.T. and El Azab, A.A. (1994): Black sand assessment. The Egyptian Geological Survey and Mining Authority, paper No.67, 48p.

Ramadohr, P. (1940): Die Erzmineralien in gewöhnlichen magmatischen Gesteinen. Abh. Preu B. Akad. Wiss. Math.-nat. kl., Nr.2, pp.1-43.

Ramadohr, P. (1956): Die Beziehungen von Fe-Ti-Erzen aus magmatischen Gesteinen. Bull. Comm. Geol. Finlande 173, pp.1-18 (25 tables).

Straumanis, M.E.; Ejima, T. and James, W.J. (1961): The TiO_2 phase explored by the lattice constant and density method. Acta Chrystallogr., 14, pp. 493 – 497.

Temple, A.K. (1966): Alteration of ilmenite. Econ. Geol., Vol.61, pp. 695-714.

The Egyptian Black Sand's Company (1969): Project Report, Vol. I, Mineral prospecting and evaluation of ore reserves, Vol. II, Concentration, Separation and upgrading investigations. Alexandria, Egypt. Unpub. Rep.

Zaghloul, Z.M. and Kamel, K. (1966): Mineralogical and petrographical features of zircon of the black sands of Rosetta. Bull. Inst. Desert. De Egypte, Vol.16, No.1, pp.1-17.